

Excitation Spectrum for Quantum Spin Systems with Ladder, Plaquette and Mixed-Spin Structures

Akihisa Koga and Norio Kawakami

Department of Applied Physics, Osaka University, Suita, Osaka 565-0871, Japan

(October 7, 2018)

By using the series expansion techniques, we study the excitation spectrum for the two-dimensional quantum spin systems with ladder, plaquette and mixed-spin structures. We calculate the spin excitation gap and thus determine the phase boundary between the spin-gap phase and the magnetically ordered phase rather precisely. It is found that the phase diagram obtained improves fairly well the one previously obtained via the ground-state susceptibility.

I. INTRODUCTION

Two-dimensional (2D) antiferromagnetic quantum spin systems with spin gap provide a new interesting paradigm for quantum phase transitions. A typical example is the spin plaquette system such as CaV_4O_9 ,¹⁻⁹ which may be described by the 2D Heisenberg model with a plaquette structure. Another interesting example found recently is the 2D spin system composed of orthogonal spin dimers such as $\text{SrCu}_2(\text{BO}_3)_2$,¹⁰⁻¹² which may be described by the 2D Heisenberg model on a square lattice with some diagonal exchange couplings. In these 2D spin systems, the plaquette or dimer structure is essential to stabilize the non-magnetic phase with the spin gap. Concerning the spin gap formation, the topological nature of spins is also important in low-dimensional systems. In this context, mixed-spin systems have attracted considerable attention recently, in which the spatial arrangement of different spins plays a crucial role to generate the spin gap or induce an antiferromagnetic long-range order. For instance, see the references for experiments¹³ and theories¹⁴⁻¹⁸ in 1D cases.

In the previous paper,¹⁹ we have investigated the ground state quantities for the 2D spin systems with ladder, plaquette and mixed-spin structures, by extending the works^{6,8,9,20} based on the series expansion methods.²¹ Although the quantum phase transitions have been described qualitatively well, it has turned out that the obtained results lead to unsatisfactory estimates for the phase boundary in some region of the phase diagram.¹⁹ A more crucial problem raised is to what extent our series expansion correctly captures the lattice structure and/or the spin topological properties, since our expansion approach has relied on the lower-order expansions in coupling constants. Not only to resolve this problem but also to confirm our approach to be reliable, it is desirable to produce more accurate results by improving the series expansions, and also to study other quantities besides the ground state quantities.

The purpose of this work is to study the excitation spectrum for the 2D quantum spin systems with the above-mentioned structures, and clarify the role of the competing interactions in the disordered phase with the spin gap. We shall see that the excitation spectrum calculated in higher orders than the ground-state susceptibility improves the phase diagram, and at the same time confirms that our series-expansion approach indeed provides reliable results.

The paper is organized as follows. In §2, we briefly summarize how to apply the series expansion techniques²² to our systems. By performing the series expansion for the excited states²³ and employing the asymptotic analysis of power-series expansions²⁴ in §3, we obtain the dispersion relations and the phase diagram. We then discuss how the spin gap phase competes with the magnetically ordered phase for three kinds of 2D quantum spin systems mentioned above. The last section is devoted to brief summary.

II. SERIES EXPANSION METHODS

We begin by briefly summarizing the series expansion method.^{22,23} We employ here the cluster expansion around a given strong-coupling spin singlet state. Let us explain the idea taking the dimer expansion as an example.^{12,19-22,25,26} First the 2D Hamiltonian is divided into two parts: $H = H_0 + H_1$. The unperturbed Hamiltonian H_0 is composed of an assembly of isolated singlet dimers which are formed by the strong antiferromagnetic bonds. Namely, our starting configuration for the perturbation has the disordered ground state with the spin gap. We then introduce the interaction term H_1 among the independent dimers and observe how the physical quantities are changed by exploiting the power series expansion with respect to H_1 . The advantage of this cluster expansion is that we can combine analytical and numerical techniques in a complementary way. For example, the computer can be utilized to systematically generate the higher order terms from the lower ones.^{21,22} We exploit the cluster expansions which may be most appropriate for each system with different structures.

To discuss how the introduction of H_1 perturbs the disordered state with the spin gap and enhances the antiferromagnetic correlation, we calculate the dispersion relation $E(\mathbf{k})$ for 2D spin systems with various structures.¹⁹ This quantity is expanded as a power series in λ as

$$E(\mathbf{k}) = \sum_{l,m,n} a_{lmn} \cos(lk_x + mk_y) \lambda^n, \quad (1)$$

where the wave number is denoted by $\mathbf{k} = (k_x, k_y)$ and the Brillouin zone for each model will be defined in the following section. We shall calculate the dispersion relation up to the eighth order in λ for the ladder-structure system and the fifth order for both the plaquette system and the mixed-spin system. To estimate the minimum value of the dispersion relation in the first Brillouin zone, we can also expand the spin gap Δ up to the same order. Since we are not able to analyze the critical phenomena only with the obtained power-series, further asymptotic analyses are necessary to discuss the phase transitions. To this end, we make use of the Padé approximants and the differential methods²⁴ to estimate the critical point for the phase transition, the dispersion relation, etc. Especially, the critical point between the magnetically ordered and disordered phase is estimated not only by the ordinary Dlog Padé approximants but also by the biased Padé approximants. In the biased method we assume that the phase transition in our 2D quantum spin model should belong to the universality class of the 3D classical Heisenberg model.²⁷ Namely, the critical value λ_c for the perturbation parameter is determined by the formula $\Delta \sim (\lambda_c - \lambda)^\nu$ with the known exponent $\nu = 0.71$ around the transition point.²⁸ We also apply the first-order inhomogeneous differential method to the power-series to obtain the dispersion relation. It should be noted here that since higher-order coefficients in the series expansions are necessary to deduce the dispersion relation in this method correctly, we might be sometimes left with wrong values at a certain wave number after applying the asymptotic analysis. It is known that this type of pathology occasionally happens in these asymptotic approximations.²⁴ If we carefully discard this spurious behavior to find the correct one, these analyses provide a fairly good approximation in many cases, which will be explicitly shown in each case treated below.

III. EXCITATION SPECTRUM AND PHASE DIAGRAM

Let us now introduce the 2D antiferromagnetic quantum spin system defined by the Heisenberg Hamiltonian,

$$H = H_0 + H_1, \quad (2)$$

$$H_0 = J_1 \sum_{(i,j) \in G_1} \mathbf{S}_i \cdot \mathbf{S}_j, \quad (3)$$

$$H_1 = J_2 \sum_{(i,j) \in G_2} \mathbf{S}_i \cdot \mathbf{S}_j + J_3 \sum_{(i,j) \in G_3} \mathbf{S}_i \cdot \mathbf{S}_j, \quad (4)$$

where J_1 , J_2 and J_3 denote the antiferromagnetic coupling constants, and \mathbf{S}_j is the spin operator at the j -th site. To treat the mixed-spin systems as well as the ladder and plaquette systems, the spin \mathbf{S}_j is allowed to take

different values at each site. We denote the bonds (i,j) for the non-perturbed Hamiltonian as G_1 , while those for the perturbed parts as G_2 and G_3 . By appropriately choosing the set of (G_1, G_2, G_3) , we can deal with the 2D systems with various structures by the series expansion techniques. We treat below the case of $\lambda (\equiv J_2/J_1) < 1$ and $\alpha\lambda (\equiv J_3/J_1) < 1 (0 < \alpha < 1)$. In the following, the excitation spectrum is analyzed to discuss the quantum phase transitions for the 2D antiferromagnetic spin systems with ladder, plaquette and mixed-spin structures. We carry out the dimer expansion, the plaquette expansion and the mixed-spin cluster expansion. Starting with the above strong-coupling spin singlet states, we can perform the cluster expansion with respect to λ and $\alpha\lambda$.

A. Dimer expansion for ladder-structure systems

We first discuss a 2D spin system with the ladder structure, which is shown schematically in Fig. 1, where the bold, the thin and the dashed lines represent the coupling constants 1, λ_L and $\alpha_L\lambda_L$, respectively. It is noted

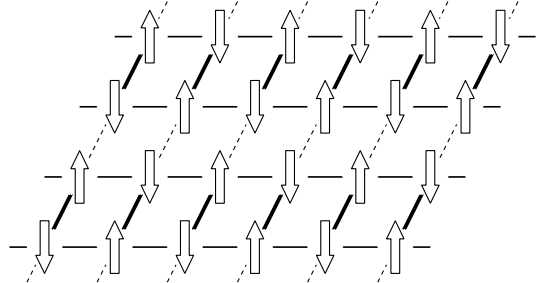


FIG. 1. The 2D $s = 1/2$ spin system with ladder structure. See the text as for the meaning of the bold, the thin, and the dashed lines.

here that the spin ladder system ($\alpha_L = 0$) was already studied in detail by the cluster expansion.²⁰ By changing α_L , we can see how the isolated 2-leg ladder ($\alpha_L = 0$) is changed to the 2D system. We calculate the energy for spin-triplet excitations by means of the dimer expansion up to the eighth order in λ_L for various values of α_L . Note that the Brillouin zone is reduced to half of the original one because the dimer singlet is composed of two spins in the y -direction. By applying the first-order inhomogeneous differential method²⁴ to the power series computed above, we obtain the spin-triplet excitation spectrum shown in Fig. 2 in the case of $\lambda_L = 0.5$. When $\alpha_L = 0$, the system is reduced to the isolated 2-leg ladders with the inter-leg (intra-leg) coupling constant 1 ($\lambda_L = 0.5$), which is known to have the disordered ground state with the spin gap.²⁹ This gives rise to the flat dispersion between $(\pi, 0)$ and $(\pi, \pi/2)$. The computed coefficients for the spin gap $\Delta = E(\pi, 0)$, in the series of λ_L are tabulated for some particular values of α_L in Table I. Note that for the isolated ladder case ($\alpha_L = 0$), our results correspond to those obtained previously by Oitmaa *et al.*²⁰ The obtained spin gap with

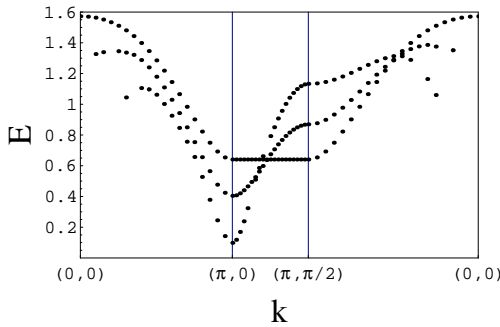


FIG. 2. Plots of the spin-triplet excitation spectrum $E(\mathbf{k})$ along high-symmetry cuts through the Brillouin zone for the system with the couplings $\alpha_L = 0.0, 0.5, 1.0$ (shown in the figure from the top to the bottom at $(\pi, 0)$, respectively) when $\lambda_L = 0.5$.

TABLE I. Series coefficients for the dimer expansion of the spin gap $\Delta = E(\pi, 0)$ for the coupled-ladder system.

n	$\alpha_L = 0.0$	$\alpha_L = 0.2$	$\alpha_L = 0.5$	$\alpha_L = 1.0$
0	1.0000000	1.0000000	1.0000000	1.0000000
1	-1.0000000	-1.1000000	-1.2500000	-1.5000000
2	0.50000000	0.38500000	0.15625000	-0.37500000
3	0.25000000	0.16025000	0.066406250	0.031250000
4	-0.12500000	-0.17002083	-0.22737630	-0.34635417
5	-0.27343750	-0.22812954	-0.26126692	-0.88050673
6	-0.15332031	-0.041639568	0.018219038	-0.16209751
7	0.24560547	0.30931367	0.36472170	-0.20085681
8	0.48133850	0.37176730	0.34136063	-0.63949210

a fixed λ_L is shown in Fig. 3. It is seen that the spin gap decreases with the increase of the inter-ladder coupling α_L and finally vanishes at which the quantum phase transition to the antiferromagnetically ordered state occurs. We wish to mention that the order in our cluster expansion is not high enough to deduce the accurate dispersion for α_L close to the transition point within the first-order inhomogeneous differential approximation, as seen in Fig. 3. It thus seems difficult to deduce the critical point α_c correctly. However, as far as the critical value is concerned, we can use alternative analysis based on the Padé approximants, which provides a rather accurate estimate for α_c , by assuming $\Delta \sim (\alpha_c - \alpha)^\nu$ near the critical point. By employing the latter analysis complementarily around the critical point α_c , we have obtained the corrected spin gap as a function of the inter-ladder coupling α_L , which is shown as the solid line in Fig. 3.

We also show the phase diagram for the coupled-ladder system in Fig. 4. The solid line represents the phase boundary obtained by the biased [4/3] Padé approximants for the spin gap, and the dashed line is the boundary determined previously by the staggered susceptibility¹⁹. It is remarkable that the present result is in fairly good agreement with the QMC simulations^{30–32} and considerably improves the previous one especially in the region with small α_L .

The above analysis may not be sufficient to discuss

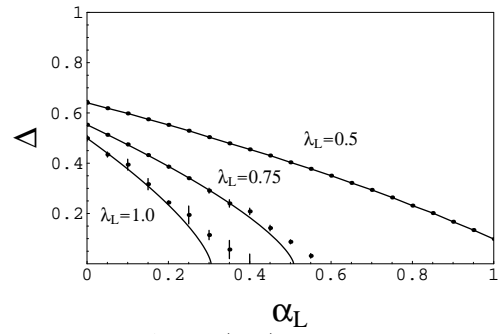


FIG. 3. Spin gap $\Delta = E(\pi, 0)$ for the coupled-ladder system in Fig. 1. The dots with error bars are the results obtained by the first-order differential method, whereas the solid lines denote the corrected values by applying the Padé approximants to the spin gap around the critical point complementarily.

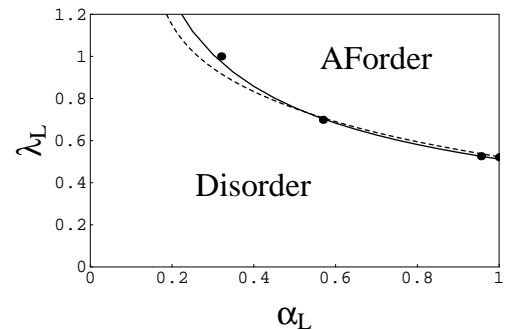


FIG. 4. Phase diagram for the coupled-ladder system in Fig. 1. The solid line indicates the phase boundary obtained by biased [4/3] Padé approximants for the spin gap while the dashed line have been obtained in our previous paper.¹⁹ The solid circles represent the results of the QMC simulations.^{30–32}

the 2D ladder-structure systems generically, because the parameter region treated by the cluster expansion is restricted. To make a complementary analysis, we next regard the present system as the coupled-dimer chains, for which the bold, the thin and the dashed lines in Fig. 1 represent the coupling constants 1, $\alpha_D \lambda_D$ and λ_D . We carry out the similar calculation up to the eighth order in α_D , and list the resulting power series for several values α_D in Table II. Applying the Padé approximants to the computed spin gap, we obtain the phase diagram shown in Fig. 5. In this figure, the solid line represents the phase boundary obtained by the biased [4/3] Padé approximants, and the dashed line is the one obtained previously by the staggered susceptibility.¹⁹ We find that these two boundaries are in fairly good agreement with each other, and furthermore consistent with those of the QMC simulations^{30,32} (the solid circles in Fig. 5). By these comparisons, we can say that our cluster expansion approach gives quite accurate results for the phase diagram.

TABLE II. Series coefficients for the dimer expansion of the spin gap $\Delta = E(\pi, 0)$ for the coupled-dimer-chain system.

n	$\alpha_D = 0.0$	$\alpha_D = 0.2$	$\alpha_D = 0.5$	$\alpha_D = 1.0$
0	1.0000000	1.0000000	1.0000000	1.0000000
1	-0.50000000	-0.70000000	-1.0000000	-1.5000000
2	-0.37500000	-0.45500000	-0.50000000	-0.37500000
3	0.031250000	0.063250000	0.062500000	0.031250000
4	-0.013020833	-0.030220833	-0.067708333	-0.34635417
5	-0.061930339	-0.10737895	-0.25710720	-0.88050673
6	0.010735971	0.040159654	0.039823179	-0.16209751
7	0.0030713964	-0.017981720	-0.12801535	-0.20085681
8	-0.031547664	-0.077754777	-0.28991249	-0.63949210

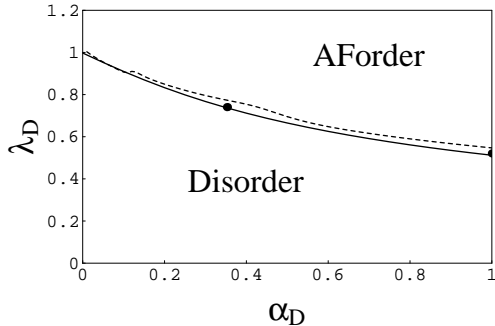


FIG. 5. Phase diagram for the coupled-dimer-chain system in Fig. 1. The solid line indicates the phase boundary obtained by the biased [4/3] Padé approximants. We also show the phase boundary which was determined by applying Dlog [4/3] Padé approximants to the fourth-order series for the staggered susceptibility.¹⁹ The solid circles represent the QMC simulation results.^{30,32}

B. Plaquette expansion

In the following, we consider the plaquette-structure systems. Introducing the spin systems with two kinds of the plaquette structures, we discuss the quantum phase transitions between the ordered and the disordered states. We note here that series expansion studies on plaquette systems have been done extensively by several groups so far,^{6,8,9,19} which we shall also compare with our results in some special cases.

1. plaquettes on a square lattice

First, we treat the plaquettes on a square lattice shown in Fig. 6. The starting Hamiltonian H_0 is composed of the isolated plaquettes, whose ground state is spin singlet with the excitation gap $\Delta = 1$. We study how the antiferromagnetic correlation develops in the presence of the inter-plaquette interaction λ and $\alpha\lambda$. In the previous paper,¹⁹ we calculated the staggered susceptibility up to the fourth order and determined the phase boundary between the magnetically ordered and the disordered states (see the dashed line in Fig. 9). We here calculate the dis-

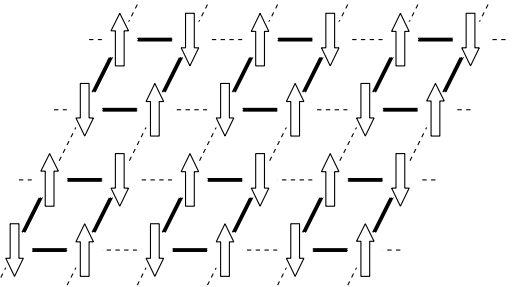


FIG. 6. Plaquette structure on a square lattice. The bold, thin, and dashed lines denote the coupling constants 1, λ , and $\alpha\lambda$ among $s = 1/2$ spins

TABLE III. Series coefficients for the plaquette expansion of the spin gap $\Delta = E(0, 0)$ for the plaquette system on a square lattice.

n	$\alpha = 0.0$	$\alpha = 0.2$	$\alpha = 0.5$	$\alpha = 1.0$
0	1.0000000	1.0000000	1.0000000	1.0000000
1	-0.66666667	-0.80000000	-1.0000000	-1.3333333
2	0.019675926	-0.068425926	-0.19762731	-0.40509259
3	0.064935378	0.016056713	-0.081316913	-0.28178048
4	0.043061549	0.019385674	-0.038615359	-0.20391542
5	0.039539538	0.030819425	-0.019630017	-0.23535878

persion for spin excitations up to the fifth order, and list the obtained series of the spin gap $\Delta = E(0, 0)$ for several values of α in Table III. Using the first-order inhomogeneous differential methods, we obtain the dispersion relation shown in Fig. 7. Note that the Brillouin zone is

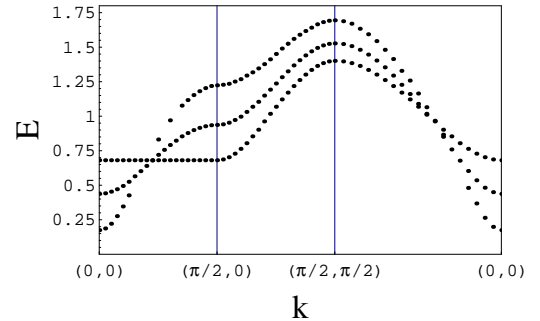


FIG. 7. Plots of the spin-triplet dispersion $E(\mathbf{k})$ along high-symmetry cuts through the Brillouin zone for the plaquette structure system with the couplings $\alpha = 0.0, 0.5, 1.0$ (shown in the figure from the top to the bottom at $(0, 0)$, respectively) in the case $\lambda = 0.5$.

reduced to a quarter of the original one due to the plaquette structure. We also show the spin gap $\Delta = E(0, 0)$ as a function of α in Fig. 8. As the inter-plaquette coupling α is increased, the antiferromagnetic correlation grows up, which causes the decrease in the excitation gap, and finally induces the quantum phase transition to the antiferromagnetic with the vanishing spin gap. In the case $(\alpha, \lambda) = (0, 1)$, our model is reduced to the independent isotropic two-leg ladders for which the spin gap $\Delta = 0.43$

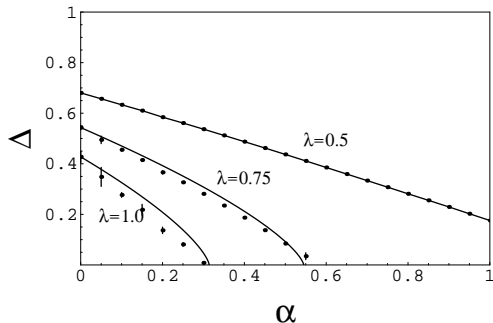


FIG. 8. Spin gap $\Delta = E(0,0)$ for the plaquette system in Fig. 6. The dots denote the results computed by the first order differential method, whereas the solid line represents those corrected with the Padé analysis around the critical point.

is obtained. This value is slightly small compared with $\Delta = 0.504$ (density matrix renormalization group)³³ and 0.5028 (dimer expansion),²⁰ which implies that higher-order cluster expansions may be necessary to obtain more accurate values of the spin gap for the plaquette system. In contrast, it is shown below that the phase diagram can be obtained with much higher accuracy. By applying Padé approximants to the power series of the spin gap, we obtain the phase diagram in Fig. 9. It is remarkable

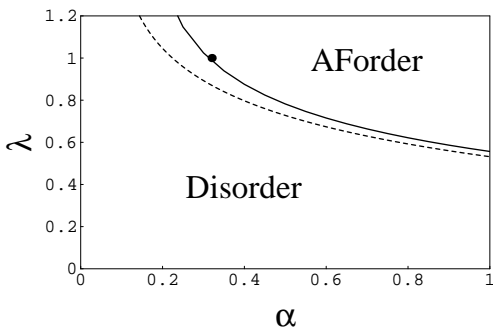


FIG. 9. Phase diagram for the plaquette system on a square lattice. The solid line indicates the phase boundary obtained by the Dlog [2/1] Padé approximants and the dashed line is the one obtained previously by the staggered susceptibility.¹⁹ The solid circles denote the QMC simulation results.³¹

that the phase boundary given in this paper considerably improves the previous one in the small α regime, which can be confirmed by the result of the QMC simulations (the dot shown in the figure).³¹ We note here that for the special case of $\alpha = 1$, similar results were previously reported by Fukumoto *et al.*⁸ and Weihong *et al.*⁹

2. plaquettes on a 1/5 depleted square lattice

We next deal with the plaquette system shown in Fig. 10, which may be regarded as a 1/5 depleted square lattice,³⁻⁵ by extending the work done by Gelfand *et al.*⁶

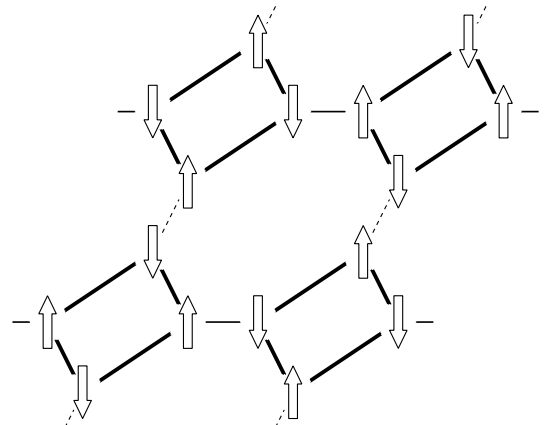


FIG. 10. 2D spin system on a 1/5 depleted square lattice. The bold, the thin, and the dashed lines indicate the coupling constants 1, λ , and $\alpha\lambda$ among $s = 1/2$ spins. For simplicity, we define the lattice constant as the distance between plaquettes.

TABLE IV. Series coefficients for the plaquette expansion of the spin gap $\Delta = E(\pi, \pi)$ for the plaquette system on a 1/5 depleted square lattice.

n	$\alpha = 0.0$	$\alpha = 0.2$	$\alpha = 0.5$	$\alpha = 1.0$
0	1.0000000	1.0000000	1.0000000	1.0000000
1	-0.33333333	-0.40000000	-0.50000000	-0.66666667
2	-0.10590278	-0.13236111	-0.18793403	-0.32291667
3	0.032959989	0.024330922	0.0092901536	-0.0081862461
4	0.024698692	0.022081937	0.020367093	0.033841824
5	-0.0070637727	-0.0088223796	-0.014159237	-0.044030516

This system is also considered to be made out of the plaquette chains,^{5,18,34,35} since the model with $\alpha = 0$ and finite λ is reduced to the isolated plaquette chains. The results for the cluster expansion of the spin gap up to the fifth order are tabulated in Table IV for several values of α . The resulting value of Δ deduced by the Padé analysis is shown in Fig. 11 as a function of α . In the case of $\alpha = 0$, the model is reduced to the isolated plaquette chains with the spin gap. In this case, by applying the differential methods to the power series, the spin gap is estimated as $\Delta = 0.607 \pm 0.001$ for $\lambda = 1$, which is in good agreement with the result of the exact diagonalization $\Delta = 0.6086$.^{5,35} To observe the phase transition when the couplings α between the plaquette chains increased, the phase diagram is shown in Fig. 12. Here, the phase boundary (solid line) is determined by applying the biased [2/3] Padé approximants to the spin gap. We find that this line is quite consistent with the previous results¹⁹ shown as the dashed line. The fact that the two lines evaluated for different quantities in different orders produce a quite similar behavior confirms that the obtained boundary is indeed reliable although our calculation is restricted to the lower-order expansions. We also note that the results already obtained by QMC⁴ and also by the plaquette expansion⁶ in the case of $\alpha = 1$ are

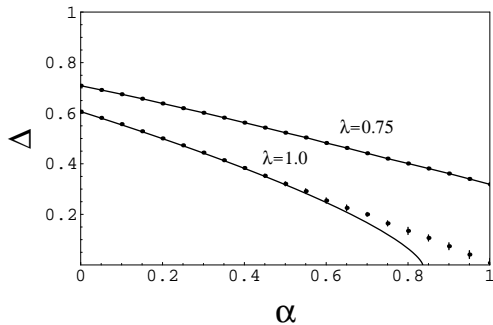


FIG. 11. Spin gap $\Delta = E(\pi, \pi)$ for the plaquette system in Fig. 6. The dots are the data computed by the first order differential method, and the solid line denotes the corrected one by combining the Padé analysis around the region with the small spin gap.

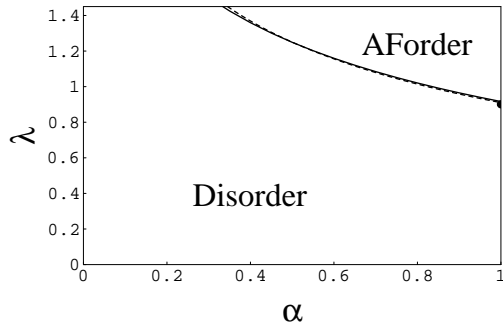


FIG. 12. Phase diagram for the plaquette system in Fig. 10. The solid line denotes the phase boundary obtained by the biased [2/3] Padé approximants while the dashed line is the previous results¹⁹ obtained by the staggered susceptibility. The solid circles denote the results of the QMC simulation.⁴

in good agreement with the present one.

C. Mixed-spin cluster expansion

Let us now turn to another interesting 2D system composed of two kind of different spins, which has attracted much attention recently. In this mixed-spin system, the topological nature of spins is important for the system to generate the spin gap or induce an antiferromagnetic long-range order. In this subsection, we extend the previous calculations¹⁹ to those of the excited states, and quantitatively discuss the phase transition in 2D mixed-spin systems. We will clarify that the arrangement of different spins affects the nature of the quantum phase transitions from the spin-gap phase to the antiferromagnetic phase. We shall also check that our series expansion approach correctly captures the spin structure though our calculation is based on the lower-order perturbations.

We deal with two typical systems composed of $s = 1/2$ and 1, as displayed in Figs. 13 and 14.¹⁹

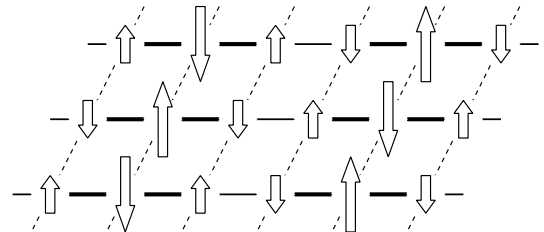


FIG. 13. 2D spin system with the *columnar*-type mixed-spin structure with $s = 1, 1/2$. We denote the coupling constants 1, λ , and $\alpha\lambda$ by the bold, the thin, and the dashed lines.

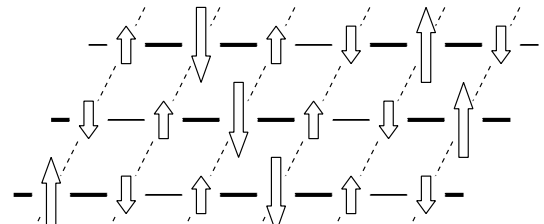


FIG. 14. 2D spin system with the *diagonal*-type mixed-spin structure. The meanings of the bold, the thin, and the dashed lines are the same as those in Fig. 13.

1. columnar-type mixed-spin system

We begin with the columnar-type mixed-spin system, for which the mixed-spin chains are stacked uniformly in a vertical direction (Fig. 13). Starting from the mixed-spin clusters of $1/2 \circ 1 \circ 1/2$, we perform the series expansion with respect to λ . Note that the Brillouin zone is reduced to a third of the original one since the mixed-spin cluster is composed of three spins in the x -direction. We list the power series obtained up to the fifth order for the excitation spectrum in Table V. It is noted that in the case of the isolated mixed-spin chain ($\alpha = 0$), these coefficients are the same as those for the plaquette chain, (see Fig. 10) and thus the isotropic mixed-spin chain with $\lambda = 1$ has the same spin gap $\Delta = 0.607$. We can indeed prove that the mixed-spin chain is identical to the plaquette chain as far as the ground state and the low-energy elementary excitation are concerned. Using the first-order inhomogeneous differential methods, we obtain the dispersion relation shown in Fig. 15. We recall

TABLE V. Series coefficients for the mixed-spin cluster expansion of the spin gap $\Delta = E(\pi/3, \pi)$ for the 2D *columnar* mixed-spin system.

n	$\alpha = 0.0$	$\alpha = 0.2$	$\alpha = 0.5$	$\alpha = 1.0$
0	1.0000000	1.0000000	1.0000000	1.0000000
1	-0.3333333	-0.7333333	-1.3333333	-2.3333333
2	-0.10590278	-0.20868056	-0.24826389	-0.008680556
3	0.032959989	-0.014472881	-0.090593252	0.50585737
4	0.024698692	0.013380005	-0.14493772	-1.8264592
5	-0.0070637727	-0.046571788	-0.44465163	-5.2417951

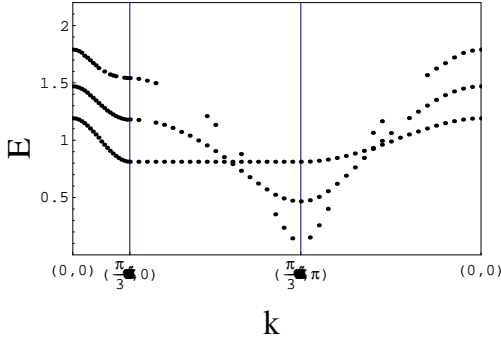


FIG. 15. Plots of the spin-triplet dispersion relation $E(\mathbf{k})$ along high-symmetry cuts through the Brillouin zone for the *columnar* mixed-spin system with the couplings $\alpha = 0.0, 0.3, 0.6$ (shown in the figure from the top to the bottom at $(\pi/3, \pi)$, respectively) in the case $\lambda = 0.5$.

that the mixed-spin system in the case of $\alpha = 0$ is reduced to the mixed-spin chain with the spin gap defined at the wave number $\mathbf{k} = (\pi/3, \pi)$. Increasing the inter-chain coupling α , we can see that the spin gap decreases as the magnetic correlation grows up, and finally vanishes at which the phase transition to the magnetically ordered phase takes place. In Fig. 16, the phase bound-

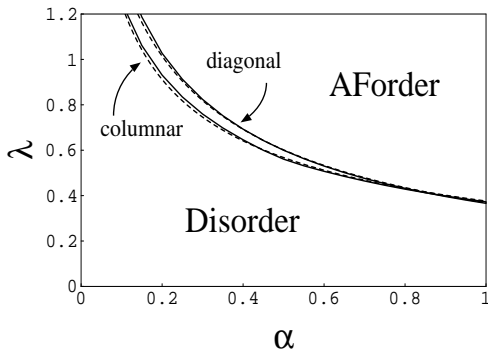


FIG. 16. The left (right) solid line represents the phase boundary for the mixed-spin system in Fig. 13 (Fig. 14). The results obtained from the ground-state susceptibility¹⁹ are shown as the dashed lines.

ary is shown by the left solid line, which is obtained by the biased [2/3] Padé approximants for the spin gap. In comparison, we also display the previous result¹⁹ by the left dashed line, which was determined by the staggered susceptibility in the fourth-order expansion. As has been the case for the plaquette systems, we can see again that the phase boundaries which were determined via the different physical quantities are consistent with each other. This demonstrates that the reliable phase boundary is established by the present analysis.

2. diagonal-type mixed-spin system

We next discuss the diagonal-type mixed-spin system shown in Fig. 14, for which the mixed-spin chains are stacked diagonally. According to this structure, the shape of the Brillouin zone for the diagonal system is quite different from those for the columnar one as shown in Fig. 17. The definition of the coupling constants is

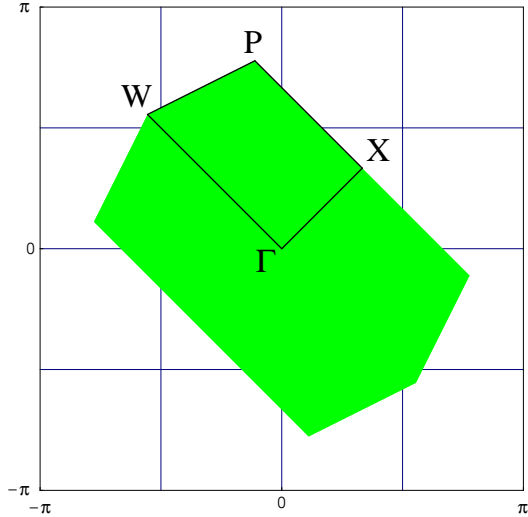


FIG. 17. First Brillouin zone for the 2D system with the *diagonal* mixed-spin structure.

the same as that in Fig. 13. The mixed-spin cluster expansion for the excited states up to the fifth order with the asymptotic analysis yields the phase diagram and the dispersion relations shown in Figs. 16 and 18, respectively. In Fig. 16, the right solid line represents the phase boundary determined by the biased [3/2] Padé approximants for the spin gap. The resulting series for

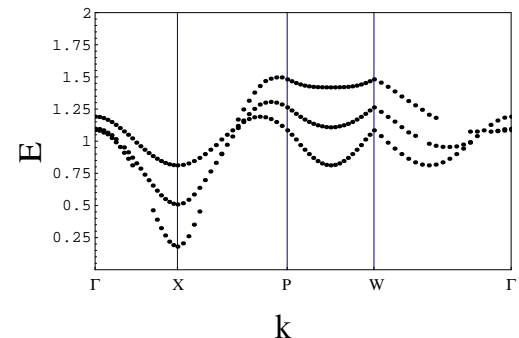


FIG. 18. Plot of the spin-triplet dispersion relation $E(\mathbf{k})$ for the *diagonal* mixed-spin system with the coupling parameters $\alpha = 0.0, 0.3, 0.6$ (shown in figure from the top to the bottom at $(\pi/3, \pi/3)$, respectively) when $\lambda = 0.5$.

some particular values of α are tabulated in Table VI. For $\alpha = 0$, the system correctly reproduces an assembly of independent mixed-spin chains which have the disordered ground state. Increasing α , the correlation among

TABLE VI. Series coefficients for the mixed-spin cluster expansion of the spin gap $\Delta = E(\pi/3, \pi/3)$ for the 2D *diagonal* mixed-spin system.

n	$\alpha = 0.0$	$\alpha = 0.2$	$\alpha = 0.5$	$\alpha = 1.0$
0	1.0000000	1.0000000	1.0000000	1.0000000
1	-0.33333333	-0.66666667	-1.16666667	-2.0000000
2	-0.10590278	-0.22430556	-0.42925347	-0.84375000
3	0.032959989	0.025971997	-0.066280914	-0.41995001
4	0.024698692	0.0053494949	-0.11649536	-0.96473863
5	-0.0070637727	-0.0082040994	0.020462458	-0.0043513404

the mixed-spin chains grows up, and the quantum phase transition occurs. Especially, in the case of the mixed-spin chains with the isotropic bonds ($\lambda = 1$), the phase transition to the ordered state occurs at the critical value $\alpha_c = 0.21$. We note that as well as the case of the columnar case, this line is consistent with the phase boundary determined from the ground-state susceptibility,¹⁹ shown as the dashed line in Fig. 16, which may ensure that phase diagrams for both of the two distinct mixed-spin systems are determined in rather high accuracy.

IV. SUMMARY

We have performed the systematic cluster expansion to study the two dimensional quantum spin systems with modulated lattice as well as spin structures. By applying the asymptotic analysis to the obtained series, we have calculated the excitation spectrum and have discussed the quantum phase transitions. We have thus constructed the phase diagram which improves the previous one obtained via the staggered susceptibility. In particular, we find that the present results for the systems with the ladder and plaquette structures are in fairly good agreement with the results of the QMC simulations. We have further studied the critical phenomena for the spin systems with modulated $S = 1, 1/2$ structure. By careful study on two types of slightly different systems with mixed-spins, it has been clarified that the topology of the spin arrangement plays an important role to stabilize the spin-gap phase.

ACKNOWLEDGEMENTS

The work is partly supported by a Grant-in-Aid from the Ministry of Education, Science, Sports, and Culture. A. K. is supported by the Japan Society for the Promotion of Science. Numerical computation in this work was carried out at the Yukawa Institute Computer Facility.

- ¹ S. Taniguchi, T. Nishikawa, Y. Yasui, Y. Kobayashi, M. Sato, T. Nishioka, M. Kontani and K. Sano: J. Phys. Soc. Jpn. **64** 2758 (1995).
- ² K. Kodama, H. Harashina, H. Sasaki, Y. Kobayashi, M. Kasai, S. Taniguchi, Y. Yasui, M. Sato, K. Kakurai, T. Mori and M. Nishi: J. Phys. Soc. Jpn. **66** 793 (1997).
- ³ K. Ueda, H. Kontani, M. Sigrist and P. A. Lee: Phys. Rev. Lett. **76** 1932 (1996).
- ⁴ M. Troyer, H. Kontani and K. Ueda: Phys. Rev. Lett. **76** 3822 (1996).
- ⁵ N. Katoh and M. Imada: J. Phys. Soc. Jpn. **64** 4105 (1995).
- ⁶ M. P. Gelfand, Z. Weihong, R. R. P. Singh, J. Oitmaa and C. J. Hamer: Phys. Rev. Lett. **77** 2794 (1996).
- ⁷ O. A. Starykh, M. E. Zhitomirsky, D. I. Khomskii, R. R. P. Singh and K. Ueda: Phys. Rev. Lett. **77** 2558 (1996).
- ⁸ Y. Fukumoto and A. Oguchi: J. Phys. Soc. Jpn. **67** 697 (1998); J. Phys. Soc. Jpn. **67** 2205 (1998).
- ⁹ Z. Weihong, J. Oitmaa and C. J. Hamer: Phys. Rev. B **58** 14147 (1998); R. R. P. Singh, Z. Weihong, C. J. Hamer and J. Oitmaa: cond-mat / 9904064.
- ¹⁰ H. Kageyama, K. Yoshimura, R. Stern, N. V. Mushnikov, K. Onizuka, M. Kato, K. Kosuge, C. P. Slichter, T. Goto and Y. Ueda: Phys. Rev. Lett. **82** 3168 (1999).
- ¹¹ S. Miyahara and K. Ueda: Phys. Rev. Lett. **82** 3701 (1999).
- ¹² Z. Weihong, C. J. Hamer and J. Oitmaa: cond-mat / 9811030.
- ¹³ G. T. Yee, J. M. Manriquez, D. A. Dixon, R. S. McLean, D. M. Groski, R. B. Flippen, K. S. Narayan, A. J. Epstein and J. S. Miller: Adv. Mater. **3** 309 (1991); Inorg. Chem. **22** 2624 (1983); Inorg. Chem. **26** 138 (1987).
- ¹⁴ S. K. Pati, S. Ramasesha and D. Sen: Phys. Rev. B **55** 8894 (1997); A. K. Kolezhuk, H.-J. Mikeska and S. Yamamoto: Phys. Rev. B **55** R3336 (1997); F. C. Alcaraz and A. L. Malvezzi: J. Phys. A **30** 767 (1997); H. Nigge-mann, G. Uimin and J. Zittartz: J. Phys. Cond. Matt.: **9** 9031 (1997).
- ¹⁵ H. J. de Vega and F. Woynarovich: J. Phys. A **25** 449 (1992); M. Fujii, S. Fujimoto and N. Kawakami: J. Phys. Soc. Jpn. **65** 2381 (1996).
- ¹⁶ T. Tonegawa, T. Hikihara, M. Kaburagi, T. Nishino, S. Miyashita and H.-J. Mikeska: J. Phys. Soc. Jpn. **67** 1000 (1998).
- ¹⁷ T. Fukui and N. Kawakami: Phys. Rev. B **55** R14709 (1997); Phys. Rev. B **56** 8799 (1997).
- ¹⁸ A. Koga, S. Kumada, N. Kawakami and T. Fukui: J. Phys. Soc. Jpn. **67** 622 (1998).
- ¹⁹ A. Koga, S. Kumada and N. Kawakami: J. Phys. Soc. Jpn. **68** 2373 (1999).
- ²⁰ J. Oitmaa, R. R. P. Singh and Z. Weihong: Phys. Rev. B **54** 1009 (1996), Z. Weihong, V. Kotov and J. Oitmaa: Phys. Rev. B **57** 11439 (1998).
- ²¹ R. R. P. Singh, M. P. Gelfand and D. A. Huse: Phys. Rev. Lett. **61** 2484 (1988).
- ²² M. P. Gelfand, R. R. P. Singh and D. A. Huse: J. Stat. Phys. **59** 1093 (1990).
- ²³ M. P. Gelfand: Solid State Commun. **98** 11 (1996).
- ²⁴ A. J. Guttmann, in *Phase Transitions and Critical Phenomena*, edited by C. Domb and J. L. Lebowitz (Academic, New York, 1989), Vol. 13.
- ²⁵ M. P. Gelfand, R. R. P. Singh and D. A. Huse: Phys. Rev.

B **40** 10801 (1989); M. P. Gelfand: Phys. Rev. B **42** 8206 (1990); I. Affleck, M. P. Gelfand and R. R. P. Singh: J. Phys. A **27** 7313 (1994).

²⁶ K. Hida: J. Phys. Soc. Jpn. **61** 1013 (1992); M. P. Gelfand: Phys. Rev. B **53** 11309 (1996); Y. Matsushita, M. P. Gelfand and C. Ishii: J. Phys. Soc. Jpn. **66** 3648 (1997); Z. Weihong: Phys. Rev. B **55** 12267 (1997).

²⁷ S. Chakravarty, B. I. Halperin and D. R. Nelson: Phys. Rev. B **39** 2344 (1989).

²⁸ M. Ferer and A. Hamid-Aidinejad: Phys. Rev. B **34** 6481 (1986).

²⁹ T. M. Rice, S. Gopalan and M. Sigrist: Europhys. Lett. **23** 445 (1993); E. Dagotto and T. M. Rice: Science **271** 618 (1996).

³⁰ N. Katoh and M. Imada: J. Phys. Soc. Jpn. **63** 4529 (1994).

³¹ M. Imada and Y. Iino: J. Phys. Soc. Jpn. **66** 568 (1997).

³² Y. Nonomura also studied this system by means of QMC simulations, (unpublished)

³³ S. R. White, R. M. Noack and D. J. Scalapino: Phys. Rev. Lett. **73** 886 (1994).

³⁴ N. B. Ivanov and J. Richter: Phys. Lett. **232A** 308 (1997).

³⁵ J. Richter, N. B. Ivanov and J. Schulenburg: J. Phys. Condence Matt. **10** 3635 (1998).